PERGAMON

Solid State Communications 115 (2000) 213–216

solid state communications

www.elsevier.com/locate/ssc

Neutron diffraction study of metamagnetic phases in $ErNi_2B_2C$

A.J. Campbell[a], D.McK. Paul[a,*], G.J. McIntyre[b]

[a]*Department of Physics, University of Warwick, Coventry, CV4 7AL, UK*
[b]*Institut Laue-Langevin, B.P. 156, 38042 Grenoble Cedex 9, France*

Received 24 February 2000; accepted 15 March 2000 by R.T. Phillips

Abstract

Neutron diffraction has been used to determine the magnetic order in the metamagnetic phases of $ErNi_2B_2C$, with the magnetic field applied parallel to the [0 1 0] and [1 1 0] crystallographic axes. Below 6 K, $ErNi_2B_2C$ has an incommensurate antiferromagnetic structure with a modulation along the *a*-axis of wavevector $\delta = (0.55, 0, 0)$. For both orientations three first-order metamagnetic transitions are observed below 6 K as the applied field is increased. The first two transitions are to incommensurate antiferromagnetic states with different values of the *a*-axis modulation, and the third transition is to a saturated paramagnetic state in which the spins are aligned ferromagnetically by the applied field. With the field applied parallel to the [0 1 0] direction, which is the magnetically easy axis, the upper incommensurate state has an additional ferromagnetic component which is not observed with the field applied parallel to the [1 1 0] direction.

Keywords: A. Magnetically ordered materials; A. Superconductors; D. Phase transitions; E. Neutron scattering

The family of superconducting compounds of the form $RENi_2B_2C$ (RE = rare earth) has been the subject of considerable investigation since their discovery [1–4]. Of particular interest are those members of the family that contain magnetic rare-earth ions (such as Er, Ho, Dy), as they provide an opportunity to study the interplay between magnetism and superconductivity. Measurements on $HoNi_2B_2C$ [5–7] have shown a strong coupling between the two phenomena. In contrast, the coupling in $ErNi_2B_2C$ appears to be considerably weaker. $ErNi_2B_2C$ has a superconducting transition at about 10.5 K and orders antiferromagnetically below about 6 K (T_N). Although the onset of magnetic ordering is accompanied by a by small change in H_{C2}, it is not a deep minimum as in the case of $HoNi_2B_2C$. The magnetic structure of this state has been determined by neutron diffraction [8,9] and found to be an incommensurate spin density wave (SDW) state with modulation wavevector $\delta = [0.5526, 0, 0]$. The formation of a ferromagnetic component below 2.3 K has been proposed by Canfield et al. [10]. The magnetic and electrical properties of $ErNi_2B_2C$ have been found to be highly anisotropic. Canfield and Bud'ko [11] have observed metamagnetic transitions in this compound with the field applied in the *a*–*b* plane and determined their angular dependences. They found evidence for four different phases. Here we report neutron diffraction measurements to determine the magnetic structure of these phases in $ErNi_2B_2C$. Similar measurements on $HoNi_2B_2C$ have been reported elsewhere [7]. Neutron diffraction is an ideal technique for such studies as it allows a direct measurement of the magnetic modulations whereas magnetisation experiments only allow measurement of the net moment along the direction of the applied field.

The sample used in our experiment was a single crystal of $ErNi_2B_2C$, grown using a Ni_2B flux technique which has been well documented elsewhere [5]. The boron isotope, B^{11}, was used to reduce neutron absorption. Magnetisation measurements were carried out as a function of temperature and field using a vibrating sample magnetometer. These showed that our sample had transition temperatures in good agreement with those reported [11] and confirmed the occurrence of the metamagnetic transitions below T_N.

Neutron diffraction measurements were carried out on the thermal neutron normal-beam diffractometer, D15, of the reactor source at the Institut Laue-Langevin, in Grenoble, France, with a beam of wavelength 1.17 Å from a Cu [3 3 1] monochromator. The sample was mounted in a 4.6 T vertical cryomagnet and the field was applied parallel to the [0 1 0] and [1 1 0] crystallographic directions in order to investigate all the metamagnetic phases in this field range. The phase diagrams in each orientation were mapped out by

* Corresponding author.

0038-1098/00/$ - see front matter
PII: S0038-1098(00)00142-3

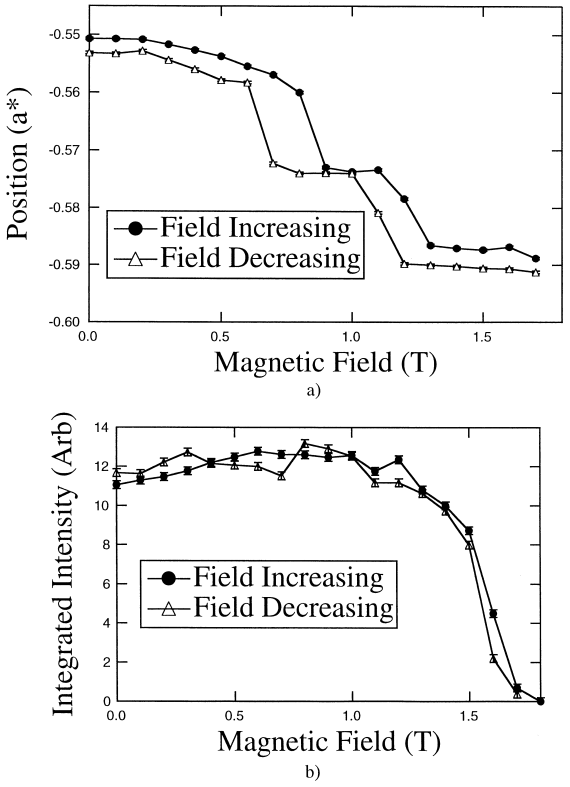

Fig. 1. a) Position and b) integrated intensity of the incommensurate magnetic reflection [−0.55 0 2] in $ErNi_2B_2C$ as a function of applied magnetic field at 2 K with the field applied parallel to the [1 1 0] crystallographic direction. The position shows metamagnetic transitions at 0.85 and 1.27 T as the field is increased. Both transitions are first order as indicated by the hysteresis.

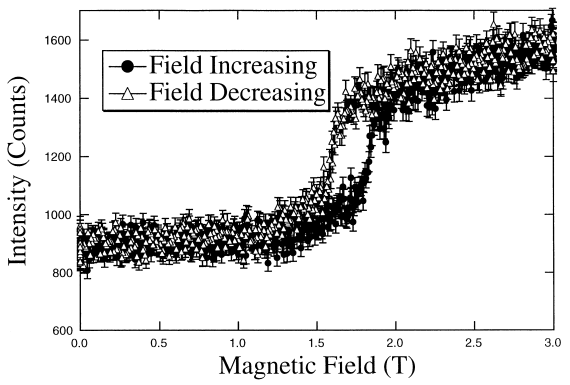

Fig. 2. Peak intensity of the [0 0 2] reflection in $ErNi_2B_2C$ as a function of applied magnetic field at 2K with the field applied parallel to the [1 1 0] crystallographic direction. The increase in intensity at 1.8 T shows the transition to a state with an increased ferromagnetic component. The transition is first order.

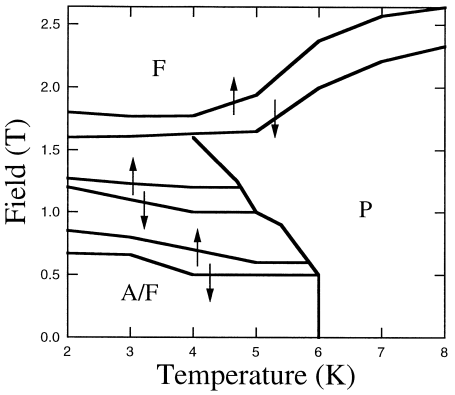

Fig. 3. Metamagnetic phase diagram of $ErNi_2B_2C$ in the plane of temperature and magnetic field with the field applied parallel to the [1 1 0] crystallographic direction. The phase marked F is a saturated paramagnetic phase in which all the spins are held parallel by the applied field. In the region marked A/F the sample has an incommensurate antiferromagnetic structure. Within this region there are phases with different values of the *a*-axis modulation. The phase P is paramagnetic. All transitions are first order. The solid and dashed lines are a guide to the eye and the arrows indicate the direction of field sweep.

following the intensity and position of an incommensurate reflection as a function of field at constant temperature and the intensity of a weak fundamental reflection. Within each phase we made scans along various reciprocal-space directions to detect possible (additional) antiferromagnetic modulations. A temperature scan was performed on a reflection characteristic of each phase, in both the increasing and decreasing field cycles, to establish the temperature phase boundaries. Finally, most accessible commensurate, and, where appropriate, incommensurate, reflections were scanned at fixed conditions in each phase to allow a refinement of the nuclear and magnetic structures. Full details of the refinements will be presented elsewhere; here we present the principal results that characterize the phase diagram.

Initially the sample was mounted with the [1 1 0] crystallographic direction parallel to the field ($\theta = 45°$ in the notation of Canfield and Bud'ko [11]. Scans above the magnetic ordering temperature showed that the sample was of excellent quality and, as expected, had a body-centred tetragonal structure (space group I4/mmm) resulting in nuclear reflections at $h + k + l = 2n$ reciprocal lattice points only. Measurements at lower temperatures to determine the zero-field magnetic structure(s) were then made, and were in good agreement with those previously reported. In order to detect any possible ferromagnetic components, the intensity of the [0 0 2] reflection was followed while decreasing the temperature. We found no evidence for the proposed [10] ferromagnetic component below 2.3 K. The temperature was then set to 2 K and the intensity and position of the incommensurate peak and the intensity of the [0 0 2] peak were measured while varying the magnetic field.

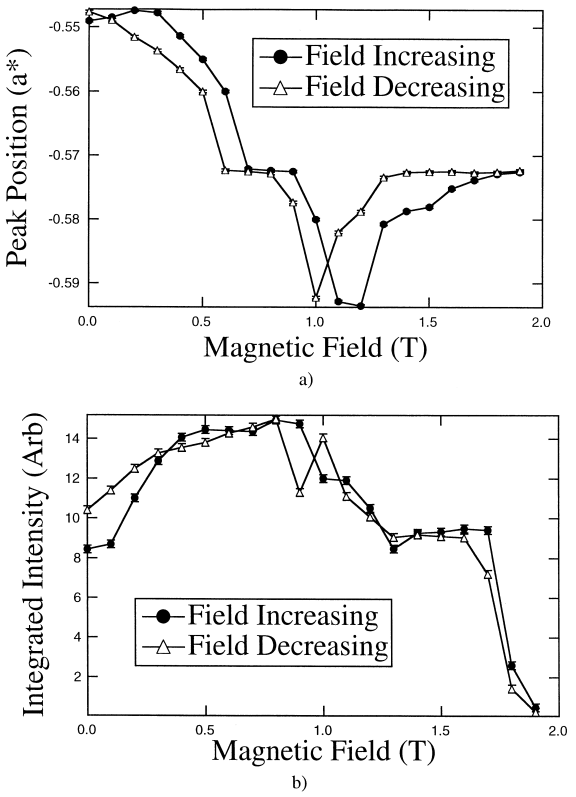

Fig. 4. a) Position and b) integrated intensity of the incommensurate magnetic reflection [−0.55 0 2] in $ErNi_2B_2C$ as a function of applied magnetic field at 2 K with the field applied parallel to the [0 1 0] crystallographic direction. Metamagnetic transitions are clearly observed at 0.4 and 1.1 T. Both transitions are first order. The intensity also shows a sharp decrease at 1.1 T.

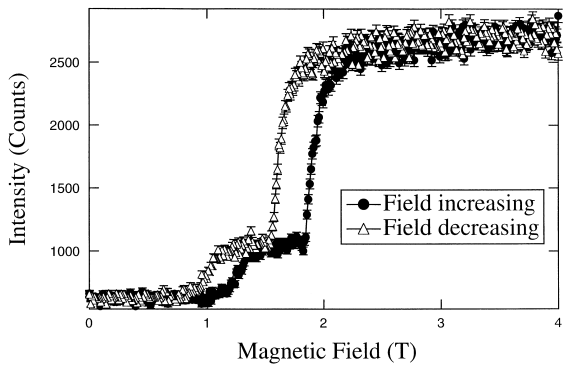

Fig. 5. Peak intensity of the [1 0 1] reflection as a function of applied magnetic field at 3 K with the field applied parallel to the [0 1 0] crystallographic direction. Metamagnetic transitions are clearly observed at 1.1 and 1.9 T. Both transitions are first order.

Fig. 1 shows a) the position and b) the integrated intensity of the incommensurate peak as a function of applied field at 2 K. Metamagnetic transitions can be seen in the peak position at 0.85 and 1.27 T. Above ~1.8 T the incommensurate peak disappears and there is a transition to a state with only a ferromagnetic component as illustrated by Fig. 2, which shows the peak intensity of the [0 0 2] peak as a function of applied field. All three transitions are first-order and occur at fields that agree with the magnetisation observations of Canfield and Bud'ko [11]. The [0 0 2] reflection was followed up to a field of 4.6 T and scans were performed in the a^* and c^* directions through various reciprocal lattice points to look for evidence of the further transition observed by Canfield and Bud'ko [11]. No further transition was found but with the applied field at this angle the critical field for this transition is very high and it is possible that we did not reach high enough fields to observe this transition. Similar field sweeps were performed at other temperatures in order to map out the phase diagram which is shown in Fig. 3.

The sample was then aligned in the cryomagnet with the [0 1 0] crystallographic direction vertical ($\theta = 0°$ in the notation of Canfield and Bud'ko [11]), and was cooled to 2 K. As for the first orientation, the intensity and position of the incommensurate peak were followed as a function of applied field. Fig. 4 shows a) the position and b) the integrated intensity of the incommensurate peak as a function of applied magnetic field at 2 K. Metamagnetic transitions are clearly observed at 0.4 and 1.1 T. However this orientation shows some significant differences compared to the previous one. After the second transition the position of the satellite does not remain constant as before, but steadily decreases showing that the wavevector of the modulation is decreasing as the applied field increases in this region. The intensity also shows a significant drop at the second transition whereas with [1 1 0] parallel to the field it decreased only slightly and smoothly through both transitions. The peak intensity of the [1 0 1] commensurate peak was also measured as a function of the field at 2 K. The results are shown in Fig. 5. The intensity shows a large increase at 2.0 T, which is where the intensity of the incommensurate peak disappears. This shows a transition from the incommensurate magnetic structure to a saturated paramagnetic structure in which the spins are held parallel by the applied field. These observations are similar to those with the [1 1 0] crystallographic direction parallel to the applied field. However, there is also an increase in the intensity of the commensurate peak at 1.1 T at the first metamagnetic transition. This shows that the second incommensurate phase includes a ferromagnetic component in addition to the incommensurate antiferromagnetic component at zero field. This increase in ferromagnetic intensity occurs at 1.1 T where the intensity of the incommensurate peak shows a sharp decrease. The decrease in the wavevector of the *a*-axis modulation above this field may also be related to this ferromagnetic component. In $ErNi_2B_2C$ the magnetic

easy axis is the *a*(*b*)-axis. In the second orientation the field is applied along the easy axis which may explain the ferromagnetic component of the second incommensurate state in this orientation. Again a set of appropriate reflections from each phase was measured to determine fully the magnetic structure in all the phases. Unfortunately there was not enough time to map out the phase diagram for this orientation of the crystal relative to the applied field. This will be completed in future measurements.

In summary, we have characterised the metamagnetic phase transitions in $ErNi_2B_2C$ for two different orientations of the crystal lattice relative to the applied field. In both orientations three first-order transitions are observed, the first two being to incommensurate antiferromagnetic states with different values of the *a*-axis modulation compared to the zero-field incommensurate state, the third transition to a saturated paramagnetic state in which the spins are held parallel by the applied field. With the field applied parallel to the [0 1 0] direction, which is the magnetically easy axis, the upper incommensurate state has a ferromagnetic component.

Future studies will continue and extend this work to look at other orientations of the crystal relative to the applied field and at metamagnetic phases in other $RENi_2B_2C$ compounds.

References

[1] R. Nagarajan, et al., Phys. Rev. Letts 72 (1994) 274.
[2] R.J. Cava, et al., Nature 367 (1994) 252.
[3] T. Siegrist, et al., Nature 367 (1994) 254.
[4] R.J. Cava, et al., Nature 367 (1994) 146.
[5] C.V. Tomy, et al., Physica B 213–214 (1995) 139.
[6] C.D. Dewhurst, et al., Phys. Rev. Letts 82 (1999) 827.
[7] A.J. Campbell et al., Phys. Rev. B, 61 (2000) 5872.
[8] S.K. Sinha, et al., Phys. Rev. B 51 (1995) 681.
[9] J. Zarestky, et al., Phys. Rev. B 51 (1995) 678.
[10] P.C. Canfield, et al., Physica C 262 (1996) 249.
[11] P.C. Canfield, S.L. Bud'ko, Journal of Alloys and Compounds 262–263 (1997) 169.